ARTHRITIS & RHEUMATISM
Vol. 63, No. 9, September 2011, pp 2721–2731
DOI 10.1002/art.30335

Chondromodulin 1 Stabilizes the Chondrocyte Phenotype and Inhibits Endochondral Ossification of Porcine Cartilage Repair Tissue

Patricia Klinger,[1] Cordula Surmann-Schmitt,[2] Matthias Brem,[3] Bernd Swoboda,[2] Jörg H. Distler,[3] Hans-Dieter Carl,[2] Klaus von der Mark,[2] Friedrich F. Hennig,[3] and Kolja Gelse[1]

Objective. **To investigate the effect of chondromodulin 1 on the phenotype of osteochondral progenitor cells in cartilage repair tissue.**

Methods. **Self-complementary adeno-associated virus (AAV) vectors carrying chondromodulin 1 complementary DNA (AAV-Chm-1) were applied to cartilage lesions in the knee joints of miniature pigs that were treated by the microfracture technique. Alternatively, isolated porcine osteochondral progenitor cells were infected with AAV-Chm-1 or with AAV-GFP control vectors ex vivo prior to being transplanted into cartilage lesions in which the subchondral bone plate was left intact. The quality of the repair tissue and the degree of endochondral ossification were assessed by histochemical and immunohistochemical methods. The effects of chondromodulin 1 overexpression were also analyzed by angiogenesis assays and quantitative reverse transcriptase–polymerase chain reaction.**

Results. **AAV-Chm-1–infected cells efficiently produced chondromodulin 1, which had strong antiangiogenic effects, as verified by the inhibition of tube formation of endothelial cells. Gene expression analyses in vitro revealed the cell cycle inhibitor $p21^{WAF1/Cip1}$ as one target up-regulated by AAV-Chm-1. Direct application of AAV-Chm-1 vectors into microfractured porcine cartilage lesions stimulated chondrogenic differentiation of ingrowing progenitor cells, but significantly inhibited terminal chondrocyte hypertrophy, the invasion of vessel structures, and excessive endochondral ossification, which were otherwise observed in untreated lesions. Indirect gene transfer, with infection of porcine osteochondral progenitor cells by AAV-Chm-1 ex vivo, also supported chondrogenic differentiation of these transplanted cells. AAV-Chm-1–infected cells maintained a chondrocyte-like phenotype and formed a hyaline-like matrix that was superior to that formed by uninfected or AAV-GFP–infected cells.**

Conclusion. **Our findings indicate that the antiangiogenic factor chondromodulin 1 stabilizes the chondrocyte phenotype by supporting chondrogenesis but inhibiting chondrocyte hypertrophy and endochondral ossification.**

Articular cartilage is an avascular, bradytrophic tissue in which the chondrocytes physiologically maintain their unique differentiation status throughout life. In contrast to chondrocytes of the fetal growth plate, articular chondrocytes are postmitotic cells that do not undergo terminal differentiation, and their extracellular matrix does not calcify above the tidemark. Bone marrow–stimulating techniques, such as microfracturing of the subchondral bone plate, are simple, minimally invasive, and cost-effective cartilage repair approaches that are frequently applied in clinical settings. Unfortunately, the ingrowing osteochondral progenitor cells often fail to undergo complete chondrogenic differentiation, which leads to the formation of inferior fibrocar-

Supported by the Interdisciplinary Center of Clinical Research at University Hospital Erlangen (IZKF grant A36) and by the DFG (grant GE 1975/2-1). Dr. Distler's work was supported by a Career Support Award of Medicine from the Ernst Jung Foundation.

[1]Patricia Klinger, PhD, Kolja Gelse, MD: University Erlangen–Nuremberg and University Hospital Erlangen, Erlangen, Germany; [2]Cordula Surmann-Schmitt, PhD, Bernd Swoboda, MD, Hans-Dieter Carl, MD, Klaus von der Mark, PhD: University Erlangen–Nuremberg, Erlangen, Germany; [3]Matthias Brem, MD, MHBA, PhD, Jörg H. Distler, MD, Friedrich F. Hennig, MD: University Hospital Erlangen, Erlangen, Germany.

Address correspondence to Kolja Gelse, MD, Department of Orthopaedic Trauma Surgery, University Hospital Erlangen, Krankenhausstrasse 12, 91054 Erlangen, Germany. E-mail: kolja.gelse@web.de.

Submitted for publication August 31, 2010; accepted in revised form March 1, 2011.

tilage. In addition, this technique is associated with matrix calcification, vascular ingrowth, and inadvertent endochondral ossification (1–3). These negative side effects not only interfere with the clinical outcome but are also considered to be negative predictors of potential secondary salvage procedures, including autologous chondrocyte transplantation (4).

Articular cartilage contains considerable amounts of chondromodulin 1, a 25-kd glycoprotein that induces the chondrocyte phenotype and also strongly inhibits angiogenesis (5–7). Previously, we demonstrated that inferior microfracture-induced fibrocartilage is characterized by a lack of chondromodulin 1, which may be the reason for the observed matrix calcification, vascular ingrowth, and excessive ossification within the cartilage lesions (8). The aim of this study was to determine whether overexpression of chondromodulin 1 within cartilage repair tissue prevents these inadvertent effects. Due to the short half-life of recombinant proteins in vivo, and to provide a more sustained delivery of chondromodulin 1, we focused on gene transfer using self-complementary adeno-associated virus (AAV) vectors (9–11).

This study was performed using the knee joints of miniature pigs, an established cartilage repair model that is known to have poor endogenous cartilage repair responses, comparable to human joints (8,12). To evaluate the potential effects of chondromodulin 1 overexpression within the porcine cartilage lesions, we performed 2 different treatment schemes. In the first, chondromodulin 1 gene transfer was combined with the microfracture technique to capture the effects of chondromodulin 1 on ingrowing osteochondral progenitor cells. In the second, osteochondral progenitor cells were infected ex vivo with AAV vectors carrying chondromodulin 1 complementary DNA (cDNA) (AAV-Chm-1) and subsequently transplanted into chondral lesions with an intact subchondral bone plate to focus on the effect of chondromodulin 1 on transplanted osteochondral progenitor cells without the interference of invading cells from the bone marrow.

MATERIALS AND METHODS

Self-complementary AAV vectors. Human chondromodulin 1 cDNA was isolated from human chondrocytes and amplified by high-fidelity polymerase chain reaction (PCR; Fermentas). The cDNA was subcloned in the shuttle plasmid pHpa-trs-SK under the control of a cytomegalovirus promoter flanked by partial DNA sequences of the AAV serotype 2 genome (10). The resulting plasmid pscAAV-Chm-1 was used for transfection studies and was further used for construction of self-complementary AAV. AAV-Chm-1 and AAV-GFP were constructed using the triple-transfection method established by the UNC Vector Core Unit (Chapel Hill, NC) as described previously in detail (10,13).

Isolation of porcine osteochondral progenitor cells and human primary cells. For isolation of porcine autologous osteochondral progenitor cells, miniature pigs were anesthetized, and cells from the periosteum of the left tibia were isolated and cultured as described previously (14). The cells were characterized as progenitor cells as described previously (14). Human osteochondral progenitor cells were obtained from the femoral bone cavities of 4 patients undergoing total hip arthroplasty at the Division of Orthopaedic Rheumatology at the University of Erlangen–Nuremberg. Human articular chondrocytes were isolated from the dorsal femoral condyles of 4 patients undergoing total knee replacement, and cultured as described previously (15). Informed consent was obtained from each patient prior to surgery, and the institutional ethics committee approved the study protocol.

Transfection procedure and immunoblot analysis. The human immortalized chondrocyte cell line C-28a2 (established by M. B. Goldring) (16) was transfected with pscAAV-GFP or pscAAV-Chm-1 using Lipofectamine, according to the recommendations of the manufacturer (Invitrogen). Alternatively, porcine osteochondral progenitor cells were infected with AAV-GFP or AAV-Chm-1 at doses of 1,000 transducing units (TU)/cell. Supernatants were collected 4 days later and prepared as described by Kitahara et al (17). Immunoblotting was performed using goat polyclonal anti–chondromodulin 1 antibody (C-20) diluted 1:500 according to a protocol described previously (15).

Tube formation assay. Human dermal microvascular endothelial cells (HDMECs; PromoCell) were cultured in 12-well plates coated with a basement membrane matrix (Geltrex; Invitrogen). The culture medium (Dulbecco's modified Eagle's medium/Ham's F-12 and 10% fetal calf serum) was mixed at a ratio of 1:3 with the supernatants of uninfected C-28a2 cells or with those of pscAAV-Chm-1–transfected C-28a2 cells. The endothelial cells were incubated for a total of 48 hours to allow the formation of tube-like structures. Tube formation was quantified as described previously (8) by a modification of the method of Sanz et al (18). The angiogenesis index was determined for each field as the total length of connected tubes/surface of analysis. Three independent experiments were performed.

Gene expression analysis in vitro. For quantitative gene expression studies in vitro, human chondrocytes or osteochondral progenitor cells were infected with AAV-GFP or AAV-Chm-1 at doses of 1,000 TU/cell. After 2 weeks, RNA was isolated for quantitative reverse transcriptase–PCR (RT-PCR) as described previously (8). The expression levels of human chondromodulin 1, *SOX9*, $p21^{WAF1/Cip1}$, *FOXO3A*, *VEGF*, and *COL10A1* were quantified by real-time RT-PCR using the ABI Prism 7900 sequence detection system (Applied Biosystems) and Verso One-Step QRT-PCR Rox Kit (ABgene). The relative quantification of gene expression was performed by the standard curve method. For each sample, the relative amount of the target messenger RNA (mRNA) was normalized to human β_2-microglobulin (β_2m). Corresponding to its low expression levels, *COL10A1* was normalized to hypoxanthine guanine phosphoribosyltransferase. A list of the

primer and probe sets is available from the author upon request.

Preparation of cell-loaded collagen scaffolds. Six 18-month-old female adult miniature pigs (Ellegaard) with body weights of 35–40 kg were used in this study. Autologous osteochondral progenitor cells were infected with AAV-Chm-1 or AAV-GFP at doses of 1,000 TU/cell as described above. Twenty-four hours after infection, cells were transferred to the rough aspect of a bilayer type I/III collagen matrix (Geistlich Biomaterials) 48 hours prior to transplantation at a density of 2×10^6 cells/cm^2.

Surgical procedures. Three weeks after cell isolation, the animals were anesthetized, the left knee joint capsule was opened by a medial parapatellar incision, and the patella was displaced laterally. Six lesions were created in each of the animals, and each lesion was treated using one of the approaches described below. The lesions were in separate round 5-mm cartilage defects created in the central part of the femoral trochlea using a biopsy punch. All lesions were clearly separated from each other by at least 3 mm of intact cartilage as demonstrated in previous studies (8,12). The cartilage was carefully removed using a curette. Great care was taken to keep the subchondral bone plate provisionally intact.

Afterward, the prepared lesions in each of the animals were treated with the following approaches: 1) no further treatment (empty partial-thickness lesion [control]); 2) treatment with 5 microfractures (MFX) (each 1 mm in diameter and 3 mm deep) that were covered with fibrin glue (Beriplast; Aventis); 3) application of 10 μl of AAV-Chm-1 vector solution (7×10^{10} TU/ml) suspended in 10 μl fibrinogen (Beriplast) into the microfracture holes that had been cleaned of blood, followed by application of 10 μl of a thrombin solution (Beriplast) to allow gel formation and retention of the vector solution within the lesion (MFX+AAV-Chm-1); 4) transplantation of matrix-bound uninfected osteochondral progenitor cells into a nonmicrofractured lesion (matrix-associated cell transplantation [MCT]); 5) transplantation of matrix-bound AAV-GFP–infected osteochondral progenitor cells into a nonmicrofractured lesion (MCT+AAV-GFP); or 6) transplantation of matrix-bound AAV-Chm-1–infected osteochondral progenitor cells into a nonmicrofractured lesion (MCT+AAV-Chm-1).

All grafts were additionally sealed with fibrin glue to prevent cell dislocation. Among the 6 animals, the different treatment approaches were arranged in an alternating manner within the femoral trochlea. Previous studies of other miniature pigs have confirmed that no significant spatial differences exist with respect to the thickness and morphology of articular cartilage and subchondral bone within the treatment area of the femoral trochlea (8,12).

Following surgery, the animals were allowed to move freely in their cages. After 20 weeks, the animals underwent the same operation on their right knee joints as was previously performed on their left knee joints. Animals were killed 6 weeks later. This treatment scheme allowed 2 different followup periods, one of 6 weeks for the right knee joints and one of 26 weeks for the left knee joints. The knee joints were dissected, assessed macroscopically, and then prepared for histologic analysis as described below. The animal study was approved by the appropriate institutional and governmental review boards.

Histologic and immunohistologic assessment. The porcine osteochondral specimens were fixed in 4% paraformaldehyde for at least 12 hours, followed by decalcification in 0.5*M* EDTA for 3 months. After standard processing, the samples were embedded in paraffin. Serial transverse 5-μm sections of the specimens were scanned and stained with toluidine blue to estimate the proteoglycan content and with alizarin red to visualize calcified tissue and bone structures. Morphologic assessment was performed according to the International Cartilage Repair Society (ICRS) Visual Histologic Assessment Scale (19).

For immunohistochemical detection of chondromodulin 1 and CD31, deparaffinized sections were pretreated either with 0.2% hyaluronidase (Roche) for 60 minutes or with 10 m*M* Tris HCl for 5 minutes and 0.2% hyaluronidase for 15 minutes, respectively. The sections were then left to react with either rabbit anti-human chondromodulin 1 antibodies (20) diluted 1:400 or mouse anti-human CD31 monoclonal antibodies (Abcam) diluted 1:10, respectively. Negative control sections for chondromodulin 1 and CD31 were incubated with isotype normal mouse IgG (Santa Cruz Biotechnology). The sections were incubated with biotinylated anti-rabbit or anti-mouse secondary antibodies, respectively. Bound antibodies were visualized by exposure to a complex of streptavidin and biotinylated alkaline phosphatase (Vectastain ABC-AP; Vector). The sections were developed with fast red and counterstained with hematoxylin.

Immunohistochemical detection of type I, type II, and type X collagen was performed as described previously in detail (14). Briefly, all deparaffinized sections were first pretreated with 0.2% hyaluronidase for 60 minutes. For detection of type I and type II collagen, the sections were also treated with 0.2% Pronase (Sigma-Aldrich) for 60 minutes. Sections were then exposed overnight to anti-human type I collagen antibodies (MP Biomedicals) diluted 1:200, anti-human type II collagen antibodies (MP Biomedicals) diluted 1:500, or to mouse anti–type X collagen IgG (21). After incubation with a biotinylated donkey anti-mouse secondary antibody (Dianova), a complex of streptavidin and biotinylated alkaline phosphatase was added. The sections were developed with fast red and counterstained with hematoxylin.

Morphologic assessment and quantification of osseous overgrowth. For quantification of excessive bone formation, the relative volume of calcified/bone tissue within the cartilage repair tissue above the virtual line of the former subchondral bone plate was determined by point-counting histomorphometry using a grid in a modification of the method described by O'Driscoll et al (22). To determine the percentage of excessive osseous tissue within the repair tissue, 5 parallel alizarin red–stained sections separated by a distance of 1 mm throughout each of the treated lesions were captured using a Leica microscope camera and further analyzed at a magnification of 100× by a digital imaging program, as previously described in detail (8).

Detection of chondromodulin 1 expression in vivo. For the detection of transgenic chondromodulin 1 mRNA expression within the repair tissue, total RNA was isolated from a 50-mg biopsy sample obtained from the respective repair tissue using an RNeasy Mini Kit (Qiagen) and treated with DNase I for 30 minutes to remove any contaminating genomic or vector DNA, according to the recommendations

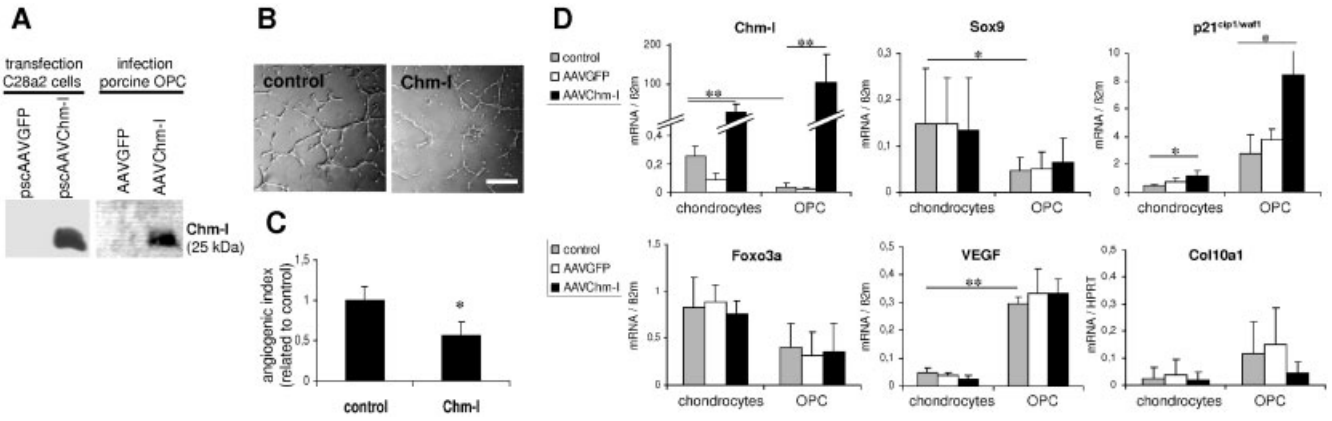

Figure 1. Functionality assessment of transgenic chondromodulin 1 (Chm-1) in vitro. **A,** Detection of chondromodulin 1 within the supernatants of C-28a2 cells transfected with psc–adeno-associated virus vectors carrying chondromodulin 1 cDNA (pscAAV-Chm-1) and of porcine osteochondral progenitor cells (OPCs) infected with AAV-Chm-1. **B,** Tube-forming capacity of human dermal microvascular endothelial cells (HDMECs), determined by angiogenesis assay. The tube-forming capacity was reduced by culturing HDMECs in a medium containing supernatants of pscAAV-Chm-1–transfected cells. Representative results from 3 independent experiments are shown. Bar = 0.5 mm. **C,** Significant reduction in the angiogenesis index after culturing HDMECs in chondromodulin 1–containing medium. Bars show the mean ± SD. $* = P < 0.05$ versus control. **D,** Expression of mRNA for chondromodulin 1, *SOX9*, $p21^{WAF1/Cip1}$, *FOXO3A*, *VEGF*, and *COL10A1*, measured by quantitative reverse transcriptase–polymerase chain reaction, in human chondrocytes and human osteochondral progenitor cells that were either uninfected (control), infected with AAV-GFP, or infected with AAV-Chm-1. Bars show the mean ± SD. $* = P < 0.05$; $** = P < 0.01$. β_2m = β_2-microglobulin; HPRT = hypoxanthine guanine phosphoribosyltransferase.

of the manufacturer. After reverse transcription, transgenic human chondromodulin 1 mRNA was detected using the primers 5′-CTGGATCACGAAGGAATCTGT-3′ and 5′-ACCATGCCCAAGATACGGG-3′ for amplification of a 180-bp fragment. A 112-bp fragment of pig β_2m mRNA, amplified by the primers 5′-CTGCTATGTATCTGGGTTCCAT-3′ and 5′-GAAAGACCAGTCCTTGCTGA-3′, was used as the internal control.

Statistical analysis. All data are presented as the mean ± SD. For the evaluation of morphologic parameters, Kruskal-Wallis nonparametric test, followed by Dunn's post hoc test multiple comparison test, was performed to determine treatment-specific differences. Excessive bone formation was assessed by analysis of variance followed by the Tukey-Kramer test. Tube formation and quantitative gene expression were analyzed using Student's 2-sided *t*-test. *P* values less than 0.05 were considered significant.

RESULTS

Validation of the gene transfer and bioactivity of transgenic chondromodulin 1. The 25-kd mature form of chondromodulin 1 was detected by specific immunoblots in the supernatants of C-28a2 cells after transfection with pscAAV-Chm-1, and in the supernatants of porcine osteochondral progenitor cells after infection with AAV-Chm-1 (Figure 1A). The bioactivity of secreted transgenic chondromodulin 1 was validated by an angiogenesis assay. Tube formation of HDMECs was strongly disturbed (Figure 1B), and the angiogenesis index of the HDMECs was significantly reduced when the cells were cultivated with conditioned medium containing secreted transgenic chondromodulin 1 in supernatants of pscAAV-Chm-1–transfected cells compared to those of pscAAV-GFP–transfected cells (control) (Figure 1C).

Results of gene expression analysis. Human chondrocytes endogenously expressed chondromodulin 1 mRNA at significantly higher levels than did human osteochondral progenitor cells (Figure 1D). In both cell types, infection with AAV-Chm-1 increased the expression of chondromodulin 1 by >1,000-fold compared with uninfected cells or cells infected with AAV-GFP control vectors. The expression of *SOX9* was significantly elevated in human chondrocytes compared with human progenitor cells, but was not influenced by overexpression of chondromodulin 1 (Figure 1D). We confirmed the up-regulation of $p21^{WAF1/Cip1}$ by chondromodulin 1 (Figure 1D), which was recently shown in cancer cell lines (23). The expression of *FOXO3A* was not influenced by chondromodulin 1. *VEGF* was more strongly expressed in human osteochondral progenitor cells than in human primary chondrocytes; however, AAV-Chm-1 infection did not influence *VEGF* mRNA levels. In contrast to progenitor cells, human articular chondrocytes hardly expressed *COL10A1*. AAV-Chm-1 infection

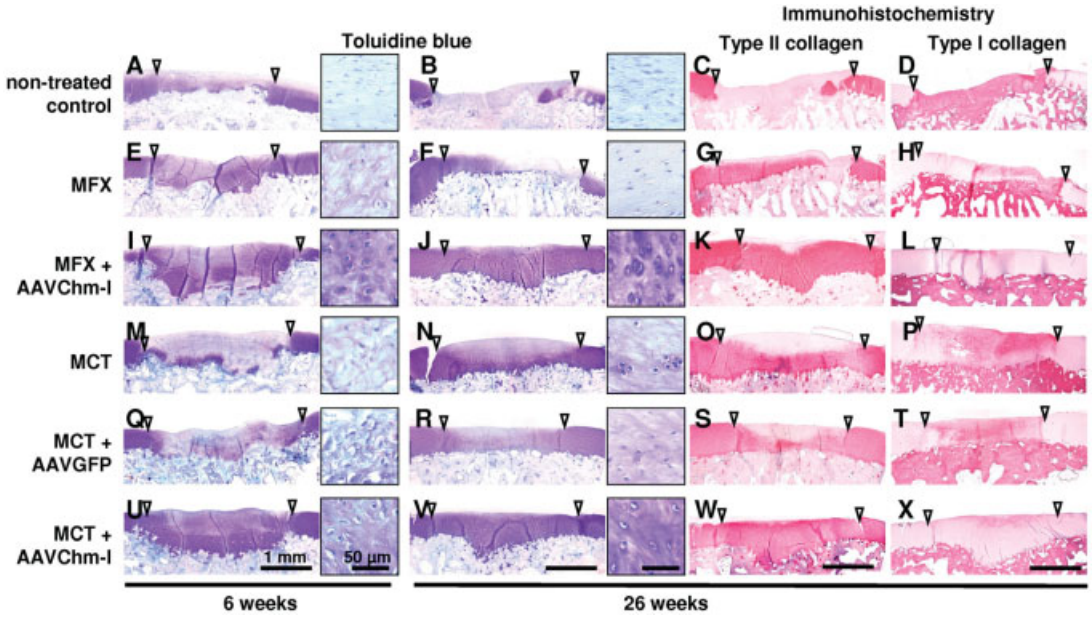

Figure 2. Porcine cartilage lesions 6 and 26 weeks after microfracturing (MFX) or matrix-associated cell transplantation (MCT). **A–D**, Toluidine blue staining (**A** and **B**) and staining for type II collagen (**C**) and type I collagen (**D**) in cartilage lesions that were left empty (untreated control). Control lesions were full of fibrous tissue that was positive for type I collagen, but negative for type II collagen. **E–H,** Toluidine blue staining (**E** and **F**) and staining for type II collagen (**G**) and type I collagen (**H**) in lesions treated by MFX. MFX failed to produce hyaline repair tissue, and was associated with subchondral bone hypertrophy. **I–L**, Toluidine blue staining (**I** and **J**) and staining for type II collagen (**K**) and type I collagen (**L**) in lesions treated by MFX and with adeno-associated virus vectors carrying chondromodulin 1 cDNA (MFX+AAV-Chm-1). Application of AAV-Chm-1 into MFX-treated defects completely inhibited excessive ossification and generated a proteoglycan-rich matrix. **M–P,** Toluidine blue staining (**M** and **N**) and staining for type II collagen (**O**) and type I collagen (**P**) in lesions treated by MCT. **Q–T,** Toluidine blue staining (**Q** and **R**) and staining for type II collagen (**S**) and type I collagen (**T**) in lesions treated with MCT+AAV-GFP. Treatment with MCT or MCT+AAV-GFP induced fibrocartilaginous repair tissue. **U–X**, Toluidine blue staining (**U** and **V**) and staining for type II collagen (**W**) and type I collagen (**X**) in lesions treated with MCT+AAV-Chm-1. Transplantation of AAV-Chm-1–infected cells resulted in a proteoglycan-rich repair matrix predominantly positive for type II collagen over type I collagen. **Insets** show higher-magnification views. **Arrowheads** indicate defect borders. Bars = 1 mm; bars in insets = 50 μm.

reduced *COL10A1* mRNA expression in progenitor cells ($P = 0.29$).

In vivo experiments and assessment of surface structure according to the ICRS Visual Histologic Assessment Scale. At 6 weeks, the untreated and MFX-treated lesions in porcine knee joints exhibited an irregular surface (Figures 2A–L). The surface structure was not significantly influenced by chondromodulin 1 gene transfer. A difference between MFX-treated and MFX+AAV-Chm-1–treated defects was observed after 26 weeks (mean ± SD ICRS score 1.8 ± 0.6 versus 2.8 ± 0.3), although it did not reach statistical significance (Table 1 and Figure 2). The use of a collagen matrix (MCT) resulted in a superior surface structure at 6 weeks compared to MFX treatment; however, such structural benefits were no longer significant at 26 weeks (Table 1). To the contrary, the use of a preformed cell-loaded matrix resulted in inadequate integration with adjacent healthy cartilage. Some remaining clefts at the defect border were still apparent after 26 weeks in 38.8% of all lesions that received a cell-loaded collagen matrix (MCT, MCT+AAV-GFP, and MCT+AAV-Chm-1) (Figures 2N, R, and V). However, such clefts were observed in only 16.6% of MFX-treated or MFX+AAV-Chm-1–treated lesions, which were not treated with a preformed matrix. Overexpression of chondromodulin 1 had no influence on the integration of the repair tissue with adjacent cartilage.

Chondrogenesis and formation of repair matrix. Both ingrowing progenitor cells from the bone marrow in MFX-treated defects (Figures 2E–H) and transplanted porcine osteochondral progenitor cells bound to a collagen matrix (MCT) (Figures 2M–P) failed to undergo complete chondrogenic differentiation. These

Table 1. Evaluation of repair tissue in porcine knee joint lesions*

Treatment	Surface	Matrix	Cell distribution	Cell population viability	Subchondral bone	Cartilage mineralization
Untreated control lesion						
6 weeks	1.6 ± 0.8	0.8 ± 0.5	0 ± 0	3 ± 0	1.6 ± 0.5	2.3 ± 1.0
26 weeks	2.0 ± 0.7	0.8 ± 0.4†	0 ± 0	3 ± 0	1.9 ± 0.7	1.8 ± 0.8
MFX						
6 weeks	1.6 ± 0.5	1.2 ± 0.5	0.3 ± 0.5	3 ± 0	1 ± 0.1	2.3 ± 0.8
26 weeks	1.8 ± 0.6	1.7 ± 0.4†	0.4 ± 0.5	3 ± 0	1.8 ± 0.4‡	1.6 ± 0.5
MFX+AAV-Chm-1						
6 weeks	1.8 ± 0.6	2.1 ± 0.9	0.3 ± 0.5	3 ± 0	1.6 ± 0.8	3 ± 0.1
26 weeks	2.8 ± 0.3	2.7 ± 0.4	0.6 ± 0.5	3 ± 0	1.9 ± 0.5	3 ± 0.1§
MCT						
6 weeks	1.8 ± 0.4	1.4 ± 0.4	0.3 ± 0.4	3 ± 0	1.8 ± 0.9‡	2.5 ± 0.5
26 weeks	2 ± 0.4	1.9 ± 0.6	0.5 ± 0.5	3 ± 0	2.1 ± 0.5	2.3 ± 0.5
MCT+AAV-GFP						
6 weeks	2.3 ± 0.3‡	1.0 ± 0.6	0.2 ± 0.4	3 ± 0	1.7 ± 0.4‡	2.6 ± 0.5
26 weeks	2.1 ± 1.0	1.5 ± 0.5†	0.5 ± 0.6	3 ± 0	1.9 ± 0.6	2.7 ± 0.3§
MCT+AAV-Chm-1						
6 weeks	2.3 ± 0.3‡	2.3 ± 0.3‡	0.7 ± 0.6	3 ± 0	1.8 ± 0.5‡	2.9 ± 0.3
26 weeks	1.9 ± 0.7	2.4 ± 0.5	0.8 ± 0.4	3 ± 0	1.8 ± 0.6	2.8 ± 0.3§
Healthy cartilage	3	3	3	3	3	3

* Values are the mean ± SD score on the International Cartilage Repair Society Visual Histologic Assessment Scale (n = 6 samples per group).
† $P < 0.05$ versus microfractured lesions 26 weeks after treatment with adeno-associated virus vectors carrying chondromodulin 1 complementary DNA (MFX+AAV-Chm-1) and versus lesions 26 weeks after treatment by transplantation of matrix-bound AAV-Chm-1–infected osteochondral progenitor cells (MCT+AAV-Chm-1).
‡ $P < 0.05$ versus MFX at 6 weeks.
§ $P < 0.05$ versus untreated control lesions at 6 weeks.

nonmodified cells rather formed inferior fibrous tissue or fibrocartilage, which was characterized by low proteoglycan content and a predominance of type I collagen (Figures 2H and P) over type II collagen (Figures 2G and O). Infection of the cells with the control vector AAV-GFP (MCT+AAV-GFP) had no impact on the quality of the repair tissue (Figures 2Q–T). In contrast, the direct application of AAV-Chm-1 (MFX+AAV-Chm-1) into microfractured lesions (Figures 2I–L) or the transplantation of AAV-Chm-1–infected porcine progenitor cells (MCT+AAV-Chm-1) (Figures 2U–X) resulted in a significantly higher quality of the repair matrix at 26 weeks compared with unstimulated MFX-treated or MCT-treated lesions without vector treatment, respectively. The repair tissue in MFX+AAV-Chm-1–treated and MCT+AAV-Chm-1–treated lesions was characterized by proteoglycan-rich matrix (Figures 2I, J, U, and V) with intense staining for type II collagen (Figures 2K and W) but only faint staining for type I collagen (Figures 2L and X).

With the exception of empty untreated defects, a certain degree of maturation of the repair tissue was observed in most MFX-treated lesions in porcine joints from 6 to 26 weeks. The changes in the matrix ICRS scores, however, did not reach significance (Table 1). Treatment with MCT+AAV-Chm-1 did not influence remodeling and maturation of the matrix within the observation period (Table 1 and Figures 2U and V). After 6 weeks, remnants of the collagen membrane could be detected in MCT-treated lesions (Figures 2M, Q, and U) with positive immunostaining for its type I collagen component (results not shown). After 26 weeks, the collagen membranes had largely been resorbed and only remnants were detectable, predominantly in superficial zones (Figures 2P, T, and X).

Zonal organization and cell viability. The zone-specific cellular distribution and zonal organization of healthy porcine articular cartilage was not achieved in any of the treatment groups within the 26-week period. Only nonsignificant tendencies for matrix remodeling could be observed in the time span between 6 and 26 weeks in most of the lesions. The repair tissue was primarily characterized by random cellular distribution without a distinct columnar organization of the cells (Figures 2B, F, J, N, R, and V and Table 1). Direct or cell-mediated AAV gene transfer or the cell transplantation itself (MCT with or without AAV-Chm-1 or AAV-GFP) did not affect the viability of the cells within the repair tissue. No pyknotic cells were detected (Table 1 and insets in Figure 2).

Chondrocyte hypertrophy and ossification. At 6 weeks, MFX-treated defects in porcine joints had disorganized granulation tissue or immature calcified tissue in subchondral areas with significantly lower "subchon-

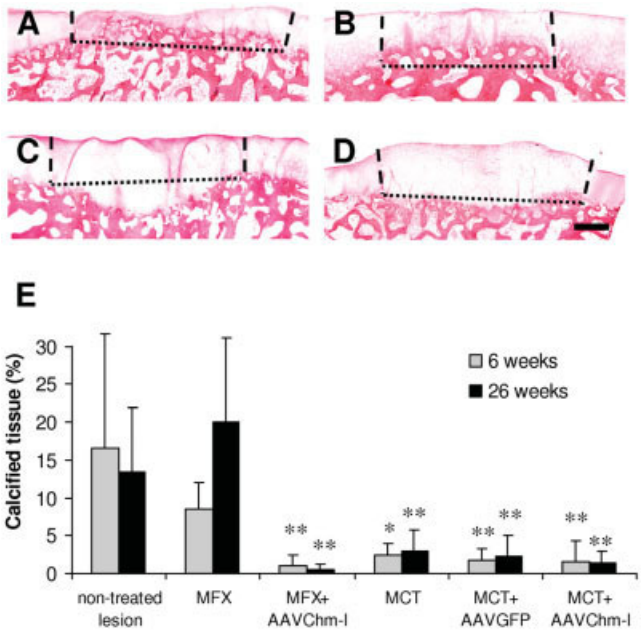

Figure 3. Evaluation of matrix calcification and excessive ossification in porcine knee joint lesions. **A–D**, Alizarin red staining to visualize calcified tissue 26 weeks after surgery in untreated lesions (**A**), lesions treated by MFX (**B**), lesions treated by MFX and with AAV-Chm-1 (**C**), and chondral defects treated with transplanted perichondrial cells modified by AAV-Chm-1 gene transfer (**D**). Dotted lines delineate the level of the original subchondral bone plate; broken lines delineate the borders of the lesions. Bar = 0.5 mm. **E**, Percentage of calcified tissue in each treatment group. The volume fraction of osseous tissue above the level of the original subchondral bone plate was related to the total repair tissue above the original level of the original subchondral bone plate. Bars show the mean ± SD. $* = P < 0.05$; $** = P < 0.01$, versus lesions treated by MFX and evaluated at the same time point. See Figure 2 for definitions. Color figure can be viewed in the online issue, which is available at http://onlinelibrary.wiley.com/journal/10.1002/(ISSN)1529-0131.

dral bone" scores than lesions in which the subchondral bone plate had been left intact. At 26 weeks, subchondral tissue had matured to some degree, with formation of bone trabeculae and marrow spaces (Table 1). The feature "cartilage mineralization" reflects calcifications within the repair matrix above the osteochondral junction, which were partially observed in MFX-treated defects in porcine joints, but not in AAV-Chm-1–treated lesions or MCT-treated lesions in porcine joints (Table 1). Additional analysis was performed to quantitatively measure the hypertrophic reaction of the subchondral bone plate. While the subchondral bone plate was still irregularly formed in MFX-treated lesions at 6 weeks (Figure 2E), excessive endochondral ossification was observed after 26 weeks (Figures 2F–H, 3B, and 3E). In MFX-treated lesions, the outgrowths of the subchondral bone plate amounted to a mean ± SD of 20.0 ± 11.1% of the volume of the repair tissue above the original subchondral bone plate (Figure 3E). Such hypertrophy of the subchondral bone plate was also present in empty untreated lesions, in which the subchondral bone plate had initially been exposed (Figures 2A–D, 3A, and 3E).

The outgrowths of bone tissue did not arise from intramembranous ossification, but rather, were a result of the endochondral ossification process, since the deepest layers of MFX-treated repair tissue were characterized by terminal chondrocyte differentiation with hypertrophic chondrocytes and strong staining for type X collagen (Figures 4A and F). At 26 weeks, those regions were replaced by osseous tissue, and only a single overlying layer of hypertrophic chondrocytes with pericellular type X collagen staining was left (Figure 4G), which indicates a cessation of the endochondral ossification process within the period of 26 weeks.

The invasion of CD31-positive vascular structures did not coincide spatially or temporally with chondrocyte hypertrophy, indicating that vascular invasion does not induce, but rather follows, chondrocyte hypertrophy (Figures 4F and K). A few CD31-positive vessel structures were observed in the middle and upper regions of the fibrous repair tissue of MFX-treated lesions, which did not coincide with chondrocyte hypertrophy (Figures 4K and P).

In contrast, chondrocyte hypertrophy with pericellular type X collagen staining and excessive bone formation was nearly completely absent in MFX-treated lesions in porcine joints both 6 and 26 weeks after treatment with AAV-Chm-1 (Figures 2I–L, 3C, 4C, and 4D). Only a single layer of cells in the deep zone showed pericellular type X collagen staining (Figures 4H and I), which was comparable to the deepest calcified layer of healthy porcine articular cartilage below the tidemark (Figure 4J). We did not detect any staining for type X collagen in superficial zones, either within the repair tissue or within healthy cartilage (results not shown). CD31-positive vessel structures were completely absent in the cartilaginous repair tissue of MFX+AAV-Chm-1–treated defects (Figures 4M and N) and in healthy cartilage (Figure 4O) and were only found below the osteochondral junction. High-magnification images showed blood vessel structures in lacunae within the subchondral bone marrow space (Figures 4Q–U).

In the MCT-treated lesions, the subchondral bone plate was left intact during surgery, and it basically retained its physiologic structure throughout the observation period. Neither relevant hypertrophy nor hypotrophy was observed (Figures 2M–P), and the infection of transplanted cells with AAV-GFP did not change the

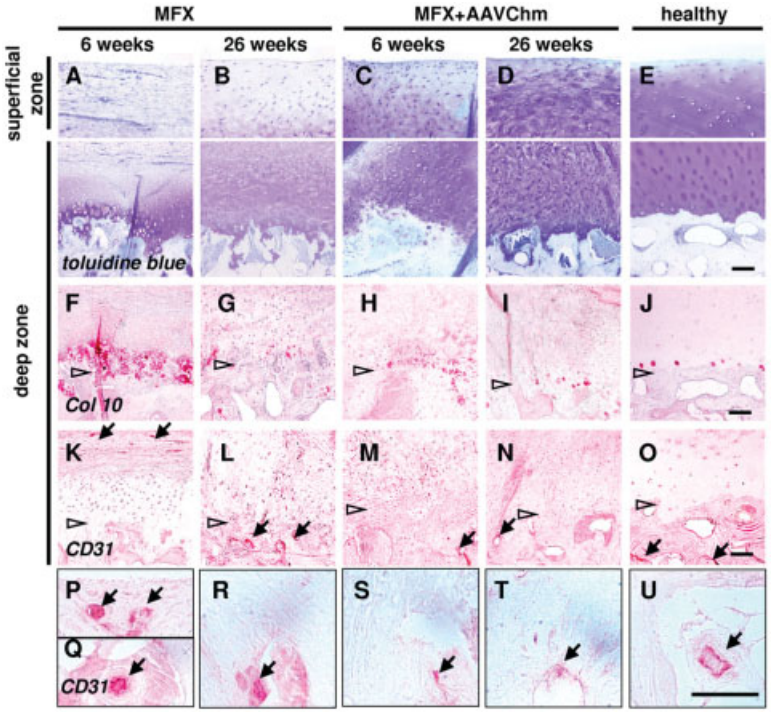

Figure 4. Detection of chondrocyte hypertrophy and vascularity in superficial and deep zones of the repair tissue in porcine knee joint lesions 6 and 26 weeks after treatment by microfracturing (MFX) or by MFX and with adeno-associated virus vectors carrying chondromodulin 1 cDNA (MFX+AAV-Chm-1) and in healthy porcine articular cartilage. **A–E,** Toluidine blue staining. Hypertrophic chondrocytes were observed, particularly in the deepest zones of MFX-treated lesions at 6 weeks. **F–J,** Type X collagen (Col 10) staining. The presence of hypertrophic chondrocytes in MFX-treated lesions was confirmed by abundant immunostaining for type X collagen. In AAV-Chm-1–treated lesions and healthy cartilage, type X collagen was only present pericellularly in the deepest cartilaginous cell layer. **K–O,** Immunostaining for CD31-positive vessel structures (**arrows**) in superficial fibrous tissue of MFX-treated defects (**K**) and in subchondral bone marrow spaces (**L–O**), but not in hypertrophic cartilage or hyaline-like repair cartilage. **P–U**, Higher-magnification views of **K–O**. Both **P** (superficial zone) and **Q** (subchondral bone space) are higher-magnification views of **K**. **Arrowheads** indicate the osteochondral junction. Bars = 50 μm. Color figure can be viewed in the online issue, which is available at http://onlinelibrary.wiley.com/journal/10.1002/(ISSN)1529-0131.

original structure of the subchondral bone (Figures 2Q–T). The transplantation of chondromodulin 1–infected cells rather tended to displace the subchondral bone plate to a deeper level (Figures 2U–X). Generally, the volume of calcified tissue in the porcine joints treated with MCT was significantly lower than that in the MFX-treated or control groups, in which the subchondral bone plate was left untreated (Figure 3E).

Detection of chondromodulin within the repair tissue. Chondromodulin 1 protein was detected immunohistochemically in healthy porcine articular cartilage above the tidemark, but not in bone trabeculae or synovial tissue (Figures 5A, B, and E). The intensity of chondromodulin 1 staining within adjacent healthy porcine cartilage did not decrease at the defect borders (asterisks in Figures 5F and G). Fibrocartilaginous repair tissue following MFX treatment stained only weakly for chondromodulin 1 (Figure 5A), and higher magnifications of the defect borders showed a distinct contrast to adjacent healthy porcine cartilage (Figure 5F). In contrast, hyaline-like repair tissue generated by MFX+AAV-Chm-1 treatment strongly stained for chondromodulin 1 (Figure 5B). Higher magnifications of the defect border zone (Figure 5G) and the deepest

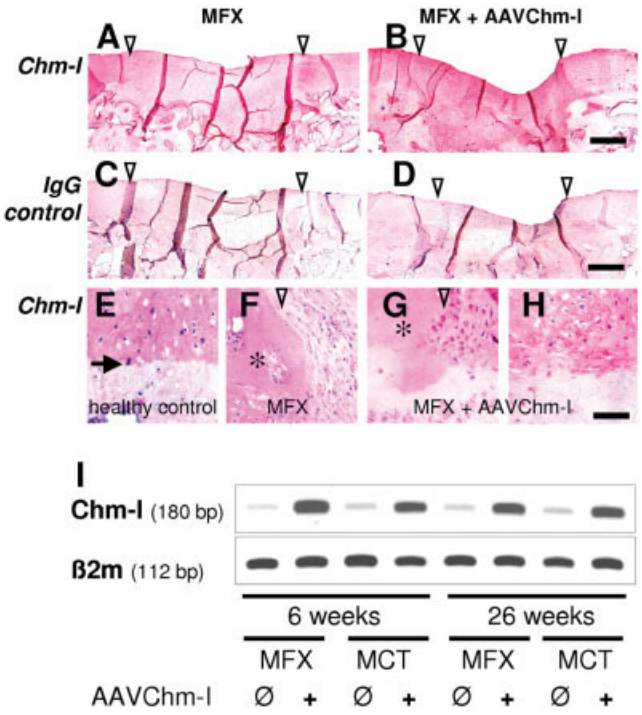

Figure 5. Detection of chondromodulin 1 (Chm-1) in the repair tissue in porcine knee joints. **A,** Chondromodulin 1 was detected by immunohistochemistry in healthy articular cartilage adjacent to the defect borders but only to a minor degree in fibrous repair tissue 6 weeks after treatment by MFX. **B,** Application of AAV-Chm-1 into microfractured lesions (MFX+AAV-Chm-1) led to strong staining for Chm-1. **C** and **D,** No nonspecific staining was evident in negative controls for Chm-1, which were incubated with isotype normal rabbit IgG in MFX-treated (**C**) or MFX+AAV-Chm-1–treated lesions (**D**). **E,** There was strong staining for Chm-1 in healthy articular cartilage above the tidemark (**arrow**), but no staining within subchondral bone. **F,** The defect border of the MFX-treated defect showed high levels of chondromodulin 1 in adjacent healthy cartilage (**asterisks**), but only low levels within repair tissue. **G** and **H,** Repair tissue treated by MFX+AAV-Chm-1 stained strongly for chondromodulin 1. **Arrowheads** indicate defect borders. **I,** Transgenic chondromodulin 1 mRNA expression was detected at both 6 and 26 weeks in repair tissue treated with AAV-Chm-1 in combination with MFX or MCT. Bars in **A–D** = 0.5 mm; bars in **E–H** = 50 μm. β_2m = β_2-microglobulin (see Figure 2 for other definitions). Color figure can be viewed in the online issue, which is available at http://onlinelibrary.wiley.com/journal/10.1002/(ISSN)1529-0131.

layer (Figure 5H) revealed high levels of chondromodulin 1 within the MFX+AAV-Chm-1–treated lesions that were comparable to levels in healthy porcine cartilage. Control immunostaining using normal rabbit IgG excluded any nonspecific staining (Figures 5C and D). Expression of chondromodulin 1 mRNA was detected within repair tissue that was treated by direct application of AAV-Chm-1 (MFX+AAV-Chm-1) or by transplantation of AAV-Chm-1–infected cells both 6 and 26 weeks after surgery (Figure 5I).

DISCUSSION

Cellular differentiation in cartilage repair tissue is challenged by 2 basic events. First, incomplete chondrogenic differentiation leads to the formation of fibrocartilage. Second, ingrowing osteochondral progenitor cells have the tendency to undergo terminal chondrogenic differentiation, which finally results in inadvertent endochondral ossification. Thus, it can be concluded that osteochondral progenitor cells tend to recapitulate the processes of the fetal growth plate or those of fracture callus, and rather adopt only a transient, instead of the permanent, chondrocyte phenotype (24,25). The present study confirmed observations of previous clinical and experimental studies, in which bone marrow–stimulating techniques resulted in inadvertent endochondral ossification and outgrowths of the subchondral bone plate (1,3,8).

So far, the mechanisms for maintaining the physiologically permanent phenotype of articular chondrocytes have not been identified completely and may involve the influence of a number of differentiation factors and growth factors, as well as environmental and biomechanical influences or epigenetic mechanisms (25–27).

It has been well documented that avascularity and the resulting tissue hypoxia are important for inducing the chondrocyte phenotype (28–33). Under physiologic conditions, the avascularity within cartilage tissue is believed to be retained by the presence of antiangiogenic proteins, such as thrombospondins or chondromodulin 1 (17,34,35). While articular cartilage is rich in these proteins, fibrocartilaginous repair tissue has been shown to lack these factors (8), which may consequently permit vessel structures to invade into the fibrous repair tissue induced by microfracture. Overexpression of chondromodulin 1 could prevent vascular invasion into the repair tissue, and it can be assumed that the prochondrogenic effects of chondromodulin 1 are, at least in part, mediated indirectly by retaining avascularity and tissue hypoxia.

To date, there are not much data regarding potential direct mechanisms by which chondromodulin 1 might exert its prochondrogenic effects. Chondromodulin 1 did not influence the expression of *SOX9*, a key transcription factor for chondrogenic differentiation. However, chondromodulin 1 was recently shown to directly suppress the growth of different cancer cell lines

by up-regulation of the cell cycle inhibitor $p21^{WAF1/Cip1}$ (23). We confirmed this effect on osteochondral progenitor cells with significant up-regulation of $p21^{WAF1/Cip1}$, which, however, seemed not to be mediated by the upstream-acting cell cycle regulator *FOXO3A*. Cell cycle arrest or cellular quiescence with up-regulation of p21 has been considered to be a characteristic feature of postmitotic chondrocytes and was shown to induce and stabilize the chondrocyte phenotype (36,37). On the basis of the limited followup period of this study, it could not be determined whether the cells within the repair tissue had attained a permanently stable chondrocyte phenotype that would still be maintained even after a decline in chondromodulin 1 transgene expression.

Besides the observed prochondrogenic effects, chondromodulin 1 strongly prevented chondrocyte hypertrophy and endochondral ossification, similar to a nude mouse model in which recombinant chondromodulin 1 prevented ectopically formed cartilage tissue from being replaced by bone (34). This effect of chondromodulin 1 cannot solely be ascribed to its antiangiogenic properties, since chondrocyte hypertrophy in the deep layers of MFX-treated lesions was neither spatially nor temporally associated with the invasion of vessels, and we could not demonstrate a direct interference of chondromodulin 1 with the expression of the proangiogenic factor *VEGF*.

Comparable to the processes within the growth plate, vascular invasion is a step that succeeds chondrocyte hypertrophy. To date, the molecular mechanisms by which chondromodulin 1 might prevent chondrocyte hypertrophy are still largely unknown. Albeit not significantly, overexpression of chondromodulin 1 showed a tendency to reduce the expression of *COL10A1* in cultured osteochondral progenitor cells. In a recent study, chondromodulin 1 was shown to inhibit the STAT signaling pathway (23), which is known to transactivate the expression of alkaline phosphatase (38) and type X collagen (39).

Generally, the poor repair response of microfractured lesions can primarily be attributed to the incomplete or unstable chondrogenic differentiation of ingrowing osteochondral progenitor cells and seems rather independent of adjacent articular cartilage. At least in the short-term followup period in the present study, there was no change in the levels of chondromodulin 1 or type II collagen in the porcine articular cartilage adjacent to the induced cartilage defects, and we did not observe relevant diffusion of chondromodulin 1 into the repair tissue. However, it has to be considered that the levels of chondromodulin 1 in adjacent cartilage may decrease with ongoing cartilage degeneration over time, as shown in a previous experimental osteoarthritis rat model (40). Similar to the repair tissue induced by microfracture, a lack of chondromodulin 1 in osteoarthritis may explain the chondrocyte hypertrophy and vascular ingrowth observed in degenerated joints (41,42).

In conclusion, chondromodulin 1 exerts a stabilizing effect on the chondrocyte phenotype in cartilage repair tissue. Chondromodulin 1 not only promotes chondrogenesis, but also significantly inhibits chondrocyte hypertrophy and endochondral ossification. These effects may not only be ascribed to its antiangiogenic properties and resulting tissue hypoxia, but may also involve cell cycle control and other still unknown molecular mechanisms and pathways. Future studies are needed to further identify chondromodulin 1–specific target genes, binding partners, receptor molecules, and signaling cascades in order to gain further insight into the mechanisms that are responsible for the maintenance of the permanent chondrocyte phenotype.

ACKNOWLEDGMENTS

We thank M. Pfluegner, H. Rohrmueller, and M. Gesslein for excellent technical assistance, and Prof. Dr. Yuji Hiraki (Kyoto University, Japan) for providing the anti–chondromodulin 1 antibody.

AUTHOR CONTRIBUTIONS

All authors were involved in drafting the article or revising it critically for important intellectual content, and all authors approved the final version to be published. Dr. Gelse had full access to all of the data in the study and takes responsibility for the integrity of the data and the accuracy of the data analysis.

Study conception and design. Klinger, Swoboda, Carl, von der Mark, Hennig, Gelse.

Acquisition of data. Klinger, Surmann-Schmitt, Brem, Gelse.

Analysis and interpretation of data. Klinger, Distler, Gelse.

REFERENCES

1. Mithoefer K, Williams RJ III, Warren RF, Potter HG, Spock CR, Jones EC, et al. The microfracture technique for the treatment of articular cartilage lesions in the knee: a prospective cohort study. J Bone Joint Surg Am 2005;87:1911–20.
2. Henderson IJ, La Valette DP. Subchondral bone overgrowth in the presence of full-thickness cartilage defects in the knee. Knee 2005;12:435–40.
3. Kreuz PC, Steinwachs MR, Erggelet C, Krause SJ, Konrad G, Uhl M, et al. Results after microfracture of full-thickness chondral defects in different compartments in the knee. Osteoarthritis Cartilage 2006;14:1119–25.
4. Minas T, Gomoll AH, Rosenberger R, Royce RO, Bryant T. Increased failure rate of autologous chondrocyte implantation after previous treatment with marrow stimulation techniques. Am J Sports Med 2009;37:902–8.
5. Hiraki Y, Tanaka H, Inoue H, Kondo J, Kamizono A, Suzuki F. Molecular cloning of a new class of cartilage-specific matrix,

chondromodulin-I, which stimulates growth of cultured chondrocytes. Biochem Biophys Res Commun 1991;175:971–7.
6. Hiraki Y, Kono T, Sato M, Shukunami C, Kondo J. Inhibition of DNA synthesis and tube morphogenesis of cultured vascular endothelial cells by chondromodulin-I. FEBS Lett 1997;415:321–4.
7. Shukunami C, Iyama K, Inoue H, Hiraki Y. Spatiotemporal pattern of the mouse chondromodulin-I gene expression and its regulatory role in vascular invasion into cartilage during endochondral bone formation. Int J Dev Biol 1999;43:39–49.
8. Blanke M, Carl HD, Klinger P, Swoboda B, Hennig F, Gelse K. Transplanted chondrocytes inhibit endochondral ossification within cartilage repair tissue. Calcif Tissue Int 2009;85:421–33.
9. Kay JD, Gouze E, Oligino TJ, Gouze JN, Watson RS, Levings PP, et al. Intra-articular gene delivery and expression of interleukin-1Ra mediated by self-complementary adeno-associated virus. J Gene Med 2009;11:605–14.
10. McCarty DM, Monahan PE, Samulski RJ. Self-complementary recombinant adeno-associated virus (scAAV) vectors promote efficient transduction independently of DNA synthesis. Gene Ther 2001;8:1248–54.
11. Steinert AF, Noth U, Tuan RS. Concepts in gene therapy for cartilage repair. Injury 2008;39 Suppl 1:S97–113.
12. Gelse K, Olk A, Eichhorn S, Swoboda B, Schoene M, Raum K. Quantitative ultrasound biomicroscopy for the analysis of healthy and repair cartilage tissue. Eur Cell Mater 2010;19:58–71.
13. Grieger JC, Choi VW, Samulski RJ. Production and characterization of adeno-associated viral vectors. Nat Protoc 2006;1:1412–28.
14. Gelse K, Muhle C, Franke O, Park J, Jehle M, Durst K, et al. Cell-based resurfacing of large cartilage defects: long-term evaluation of grafts from autologous transgene-activated periosteal cells in a porcine model of osteoarthritis. Arthritis Rheum 2008;58:475–88.
15. Grimmer C, Pfander D, Swoboda B, Aigner T, Mueller L, Hennig FF, et al. Hypoxia-inducible factor 1α is involved in the prostaglandin metabolism of osteoarthritic cartilage through up-regulation of microsomal prostaglandin E synthase 1 in articular chondrocytes. Arthritis Rheum 2007;56:4084–94.
16. Goldring MB, Birkhead JR, Suen LF, Yamin R, Mizuno S, Glowacki J, et al. Interleukin-1β-modulated gene expression in immortalized human chondrocytes. J Clin Invest 1994;94:2307–16.
17. Kitahara H, Hayami T, Tokunaga K, Endo N, Funaki H, Yoshida Y, et al. Chondromodulin-I expression in rat articular cartilage. Arch Histol Cytol 2003;66:221–8.
18. Sanz L, Pascual M, Munoz A, Gonzalez MA, Salvador CH, Alvarez-Vallina L. Development of a computer-assisted high-throughput screening platform for anti-angiogenic testing. Microvasc Res 2002;63:335–9.
19. Mainil-Varlet P, Aigner T, Brittberg M, Bullough P, Hollander A, Hunziker E, et al, International Cartilage Repair Society. Histological assessment of cartilage repair: a report by the Histology Endpoint Committee of the International Cartilage Repair Society (ICRS). J Bone Joint Surg Am 2003;85-A Suppl 2:45–57.
20. Hiraki Y, Mitsui K, Endo N, Takahashi K, Hayami T, Inoue H, et al. Molecular cloning of human chondromodulin-I, a cartilage-derived growth modulating factor, and its expression in Chinese hamster ovary cells. Eur J Biochem 1999;260:869–78.
21. Girkontaite I, Frischholz S, Lammi P, Wagner K, Swoboda B, Aigner T, et al. Immunolocalization of type X collagen in normal fetal and adult osteoarthritic cartilage with monoclonal antibodies. Matrix Biol 1996;15:231–8.
22. O'Driscoll SW, Marx RG, Fitzsimmons JS, Beaton DE. Method for automated cartilage histomorphometry. Tissue Eng 1999;5:13–23.
23. Mera H, Kawashima H, Yoshizawa T, Ishibashi O, Ali MM, Hayami T, et al. Chondromodulin-1 directly suppresses growth of human cancer cells. BMC Cancer 2009;9:166.
24. Steinert AF, Proffen B, Kunz M, Hendrich C, Ghivizzani SC, Noth U, et al. Hypertrophy is induced during the in vitro chondrogenic differentiation of human mesenchymal stem cells by bone morphogenetic protein-2 and bone morphogenetic protein-4 gene transfer. Arthritis Res Ther 2009;11:R148.
25. Zimmermann P, Boeuf S, Dickhut A, Boehmer S, Olek S, Richter W. Correlation of COL10A1 induction during chondrogenesis of mesenchymal stem cells with demethylation of two CpG sites in the COL10A1 promoter. Arthritis Rheum 2008;58:2743–53.
26. Lefebvre V, Smits P. Transcriptional control of chondrocyte fate and differentiation. Birth Defects Res C Embryo Today 2005;75:200–12.
27. Goldring MB, Tsuchimochi K, Ijiri K. The control of chondrogenesis. J Cell Biochem 2006;97:33–44.
28. Lafont JE, Talma S, Murphy CL. Hypoxia-inducible factor 2α is essential for hypoxic induction of the human articular chondrocyte phenotype. Arthritis Rheum 2007;56:3297–306.
29. Gelse K, Muhle C, Knaup K, Swoboda B, Wiesener M, Hennig F, et al. Chondrogenic differentiation of growth factor-stimulated precursor cells in cartilage repair tissue is associated with increased HIF-1α activity. Osteoarthritis Cartilage 2008;16:1457–65.
30. Lafont JE, Talma S, Hopfgarten C, Murphy CL. Hypoxia promotes the differentiated human articular chondrocyte phenotype through SOX9-dependent and -independent pathways. J Biol Chem 2008;283:4778–86.
31. Gelse K, Pfander D, Obier S, Knaup KX, Wiesener M, Hennig FF, et al. Role of hypoxia-inducible factor 1α in the integrity of articular cartilage in murine knee joints. Arthritis Res Ther 2008;10:R111.
32. Amarilio R, Viukov SV, Sharir A, Eshkar-Oren I, Johnson RS, Zelzer E. HIF1α regulation of Sox9 is necessary to maintain differentiation of hypoxic prechondrogenic cells during early skeletogenesis. Development 2007;134:3917–28.
33. Robins JC, Akeno N, Mukherjee A, Dalal RR, Aronow BJ, Koopman P, et al. Hypoxia induces chondrocyte-specific gene expression in mesenchymal cells in association with transcriptional activation of Sox9. Bone 2005;37:313–22.
34. Shukunami C, Hiraki Y. Role of cartilage-derived anti-angiogenic factor, chondromodulin-I, during endochondral bone formation. Osteoarthritis Cartilage 2001;9 Suppl A:S91–101.
35. Pfander D, Cramer T, Deuerling D, Weseloh G, Swoboda B. Expression of thrombospondin-1 and its receptor CD36 in human osteoarthritic cartilage. Ann Rheum Dis 2000;59:448–54.
36. Negishi Y, Ui N, Nakajima M, Kawashima K, Maruyama K, Takizawa T, et al. p21Cip-1/SDI-1/WAF-1 gene is involved in chondrogenic differentiation of ATDC5 cells in vitro. J Biol Chem 2001;276:33249–56.
37. Stewart MC, Farnum CE, MacLeod JN. Expression of p21CIP1/WAF1 in chondrocytes. Calcif Tissue Int 1997;61:199–204.
38. Mikami Y, Asano M, Honda MJ, Takagi M. Bone morphogenetic protein 2 and dexamethasone synergistically increase alkaline phosphatase levels through JAK/STAT signaling in C3H10T1/2 cells. J Cell Physiol 2010;223:123–33.
39. Ben-Eliezer M, Phillip M, Gat-Yablonski G. Leptin regulates chondrogenic differentiation in ATDC5 cell-line through JAK/STAT and MAPK pathways. Endocrine 2007;32;235–44.
40. Hayami T, Funaki H, Yaoeda K, Mitui K, Yamagiwa H, Tokunaga K, et al. Expression of the cartilage derived anti-angiogenic factor chondromodulin-I decreases in the early stage of experimental osteoarthritis. J Rheumatol 2003;30:2207–17.
41. Walsh DA, Bonnet CS, Turner EL, Wilson D, Situ M, McWilliams DF. Angiogenesis in the synovium and at the osteochondral junction in osteoarthritis. Osteoarthritis Cartilage 2007;15:743–51.
42. Von der Mark K, Kirsch T, Nerlich A, Kuss A, Weseloh G, Gluckert K, et al. Type X collagen synthesis in human osteoarthritic cartilage: indication of chondrocyte hypertrophy. Arthritis Rheum 1992;35:806–11.